



Cite this: *J. Mater. Chem. A*, 2018, 6, 11479

Recyclable thermoset shape memory polymers with high stress and energy output *via facile UV-curing*†

Ang Li,  Jizhou Fan and Guoqiang Li *

Engineering applications of current thermoset shape memory polymers are limited by three critical issues: demanding fabrication conditions (from 70 to 300 °C temperatures for hours or days), lack of reprocessability or recyclability, and low recovery stress and energy output. To address these problems simultaneously, a new UV curable and vitrimer-based epoxy thermoset shape memory polymer (VSMP) has been synthesized. A 1.1 mm thick VSMP film can be readily cured at room temperature under UV-irradiation (61 mW cm⁻²) in just 80 s. It possesses 36.7 MPa tensile strength, 230 MPa compressive strength, and 3120 MPa modulus at room temperature. It still has a compressive strength of 187 MPa at 120 °C. The covalent adaptable network (CAN) imparts the VSMP with recyclability, as reflected by two effective recycling cycles (>60% recycling efficiency). In addition, the VSMP exhibits good shape memory properties for multiple shape recovery cycles. With 20% compression programming strain, up to 13.4 MPa stable recovery stress and 1.05 MJ m⁻³ energy output in the rubbery state are achieved. With good mechanical strength, thermal stability, recyclability, and excellent shape memory properties combined with *in situ* UV-curing capabilities, the new VSMP is a promising multifunctional thermoset for engineering applications.

Received 21st March 2018
Accepted 16th May 2018DOI: 10.1039/c8ta02644k
rsc.li/materials-a

1. Introduction

One-way thermo-responsive shape memory polymers (SMPs) can deform to a temporary shape below the transition temperature (T_{trans}) and recover to their original shape above T_{trans} under proper stimuli, most popularly with heat.^{1,2} By converting another type of energy into heat, the shape memory effect can also be triggered by electrical actuation, light, and magnetic field.^{3–5} Due to the controllable shape transformation, SMPs have attracted much attention for the fabrication of electronic devices, sensors, fabrics, sealant, deployable structures, biomedical devices and self-healing composites.^{6–12} Moreover, recent studies have shown the great potential for SMPs to be used in oil drilling and aerospace transportation.^{13,14} However, most of the current SMPs are made of elastomers, hydrogels, or thermoplastic polymers, which are unable to provide sufficient mechanical strength, stiffness, durability, and recovery stress for engineering applications. Although a few high performance shape memory polymers (HPSMPs) or their composites have been reported,^{15,16} more HPSMPs are still highly desired given the large demand in heavy-duty engineering structures, such as the auto industry, construction, aerospace, *etc.*

Recent advances in HPSMPs primarily focus on increasing the mechanical properties of HPSMPs,^{17–19} but the shape recovery stress of these HPSMPs was not focused. Shape recovery stress or the energy output which quantifies the work produced during the shape recovery process is a critical parameter for HPSMPs to be used for engineering structures with multifunctionality. A real HPSMP is considered to possess both high mechanical strength and high shape recovery stress. Most of the current HPSMPs yield the recovery stress from tenths of MPa to several MPa in the rubbery state (<5 MPa), which is not adequate for heavy duty structural applications.^{20–22} A recovery stress of 7 MPa shown by SMPs is usually considered as high recovery stress output.^{23,24} It was commonly accepted that the energy input into amorphous SMPs was stored through entropy reduction and the recovery stress was produced through constrained shape recovery.²⁵ The latest study shows that a high recovery stress output and energy output can be produced through enthalpy increase if high steric hindrance or intermolecular interactions within the polymer network can be achieved, providing guidance for fabricating HPSMPs with high recovery stress.²⁶

Another limitation of current HPSMPs is their complex fabrication procedures. Zhang *et al.* have developed HPSMPs based on poly(*p*-dioxanone) which exhibits high tensile strength (up to 65 MPa), but the synthesis of the polymer needs 72 h under a nitrogen environment at 80 °C.¹⁷ Wang *et al.* have reported a HPSMP composed of polyimide with excellent tensile

Department of Mechanical and Industrial Engineering, Louisiana State University, Baton Rouge, Louisiana, USA 70803. E-mail: lguoqi1@lsu.edu

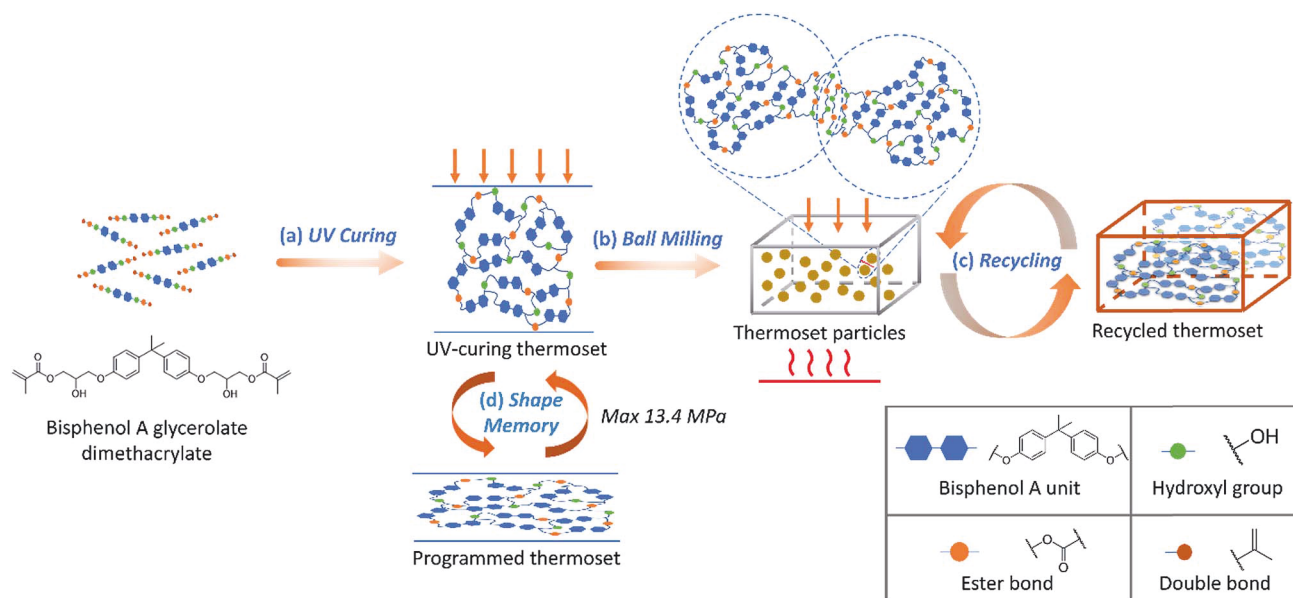
† Electronic supplementary information (ESI) available. See DOI: 10.1039/c8ta02644k

strength (up to 180 MPa), which can only be synthesized under argon at elevated temperatures (multi-step, up to 300 °C) for 31 h.¹⁸ Poly(vinyl butyral) based HPSMPs have also been developed (tensile strength up to 47 MPa), which require 24 h reaction at 70 °C.¹⁹ Despite the excellent properties, the scale-up manufacturing of HPSMPs for engineering applications is mainly impeded by complex preparation procedures and harsh fabrication conditions. A facile fabrication method is demanded to alleviate the limitations on HPSMPs. UV-curing, which usually proceeds *via* free radical polymerization or cationic polymerization, is a widely employed fabrication process in the industry.^{27,28} High heat input, time-consuming reactions, and moisture-free air protection can all be avoided through the UV-curing process. More importantly, *in situ* curing can be accomplished under UV irradiation, enabling future applications of HPSMPs as coatings and adhesives, and in stereolithography-based additive manufacturing.^{29–33} UV-curing is one of the facile methods that can be used to fabricate HPSMPs.

Chemical cross-links endow SMPs with excellent thermal stability, high mechanical strength, and good chemical resistance. However, the permanently crosslinked network makes reprocessability and recyclability impossible for polymers. Given the large demand for HPSMPs in engineering applications, the lack of recyclability brings about a big environmental concern and life cycle cost. One feasible solution is to develop vitrimer-based SMPs. Vitrimer is a type of cross-linked polymer composed of a covalent adaptable network (CAN) or reversible bonds.³⁴ In terms of the dynamic reversibility, reversible bonds have been widely incorporated in polymer networks to fabricate self-healing polymers, soft robots, and smart biomaterials.^{35–38} Most of the current vitrimer-based SMPs are made of rubber or elastomer and lack adequate mechanical strength (<4 MPa).^{39–41} The abovementioned poly(*p*-dioxanone) and poly(vinyl butyral)

based polymers are among the few reported vitrimer-based HPSMPs whose applications are significantly hindered by their complex fabrication processes.^{17,19} Efforts have been made to fabricate vitrimer-based SMPs through facile synthetic routes. Wang *et al.* synthesized a self-healing SMP composed of polybutadiene *via* UV-curing at room temperature for only 1 h.⁴² Self-healing shape memory polycaprolactone has also been prepared at room temperature under UV irradiation for 1 h.⁴³ However, the facile fabrication process has not been applied to HPSMPs.

Herein we report the development of a new high-performance UV-curable and recyclable vitrimer-based shape memory thermoset (VSMP) with high recovery stress and energy output. The design contains four factors: a rigid chain segment for high mechanical strength, acrylate/methacrylate groups for UV-curing, a CAN network for recyclability, and a highly constrained network for improved recovery stress. Therefore, bisphenol A glycerolate dimethacrylate (BPAGMA), an epoxy-based monomer, is selected. The bisphenol unit is widely existing in engineering polymers (*e.g.* polycarbonate and epoxy), providing high chain stiffness to the thermoset. The dimethacrylate group undergoes fast and complete photopolymerization under UV irradiation, leading to a highly constrained network. Moreover, the resulting ester bonds after UV-curing and the dangling hydroxyl groups form the CAN of the thermoset, enabling recyclability of the polymer. In this study, BPAGMA monomers were first UV-cured to form the new VSMP thermoset (Scheme 1(a)). To assess the recyclability, the VSMP thermoset was then broken and ground into particles through ball milling (Scheme 1(b)). A solid form recycling of the broken particles was conducted *via* an interfacial transesterification reaction to form the recycled thermoset, which can be recycled again (Scheme 1(c)). The shape memory properties of the VSMP thermoset were also



Scheme 1 (a) The VSMP is prepared by UV-curing of bisphenol A glycerolate dimethacrylate. (b) Ball milling of the VSMP into particles. (c) Recycling of the VSMP particles under pressure and with heat into a new thermoset with two effective recycling cycles. (d) Hot compressive programming of the VSMP, fixation of the temporary shape, and recovery to the original shape for multiple cycles.

demonstrated with several programming and shape recovery cycles (Scheme 1(d)).

2. Experimental section

2.1 Materials and facile UV-curing of the vitrimer-based shape memory polymer (VSMP)

Bisphenol A glycerolate dimethacrylate and 2-hydroxy-2-methylpropiophenone were purchased from Sigma-Aldrich and used as received. In this study, the photo-initiator (2-hydroxy-2-methylpropiophenone, 0.27 mL, 3 wt%) was dissolved in bisphenol A glycerolate dimethacrylate (BPAGMA, 9 g) by stirring the mixture at 65 °C for 2 h. The solution was then sandwiched between two transparent plastic slides with a PTFE spacer in between (thickness: 1.1 mm). The solution was cured in a UV chamber for a certain time (10 to 80 s) under irradiation of 61 mW cm⁻². A pale yellow but transparent specimen was then obtained by removing the plastic slides and the PTFE spacer.

2.2 Kinetic study

A series of the VSMP sheets (thickness = 1.1 mm) were synthesized for various time periods (3 s to 80 s). Each sheet sample was cut into a small piece as the specimen whose weight was measured as w_0 (120–160 mg). Each specimen was then immersed in acetone (10 mL), a good solvent for the BPAGMA monomer for 21 h under agitation. The solvent was then removed using pipettes and the immersed specimen was further dried under vacuum at 80 °C for 2 h. The conversion of polymerization

is defined as $p = \frac{\text{mole}_p}{\text{mole}_0} = \frac{\text{mole}_p \times \text{MM}_p}{\text{mole}_0 \times \text{MM}_0} = \frac{\text{mass}_p}{\text{mass}_0}$, where p stands for the conversion of polymerization, mole_p stands for the moles of polymerized monomers, mole_0 represents the moles of initial monomers, MM_p stands for the molar mass of polymerized monomers, MM_0 stands for the monomer molar mass, mass_p stands for the weight of polymerized monomers, and mass_0 stands for the weight of initial monomers. Due to the addition polymerization, there is no mass loss during the polymerization, hence, the mass of the polymerized monomers is the same as the mass of the polymer. By immersing the UV-cured VSMP in acetone, the unreacted monomers can be dissolved so that mass_p can be obtained by measuring the weight of the VSMP after immersion in acetone. On the other hand, mass_0 was obtained by measuring the weight of the VSMP after UV-curing. Therefore, the conversion of the polymerization was calculated using eqn (1):⁴⁴

$$\text{Polymerization conversion} = \frac{\text{mass}_p}{\text{mass}_0} \times 100\% \quad (1)$$

2.3 Tensile strength and compressive strength tests

Rectangular specimens (18.30 × 54.31 × 1.13 mm) were prepared for the tensile strength test using the sandwich mold mentioned before (Section 2.1). All the tensile strength tests were performed using the mechanical test system (MTS) machine (Alliance RT/5, MTS, USA) with 60 N min⁻¹ loading rate at room temperature.

Cylindrical specimens (diameter = 12.27 mm, height = 19.20 mm) were fabricated in a plastic syringe (diameter = 12.27 mm) under UV irradiation (61 mW cm⁻²) for 17 min and used for compression and subsequent shape memory tests. All the compression tests were performed using the mechanical test system (MTS) machine (QTEST 150 machine, MTS, USA) with 1 mm min⁻¹ loading rate. Both room temperature (25 °C) and elevated temperatures (75 °C, 120 °C, and 150 °C) were used to determine the compressive strength of the VSMP.

2.4 Compositional analysis, thermal analysis, and thermomechanical analysis

The compositions of the BPAGMA monomer and the UV-cured VSMP were analyzed using FTIR (Bruker Alpha FTIR Spectrometer) with the scanning range from 400 to 4000 cm⁻¹. The BPAGMA monomer with 3 wt% photoinitiator, the VSMP in powder form, and the recycled VSMP in powder form, were put in the same sample holder of the IR instrument and compressed using the holder press to ensure all three different cylindrical samples have the same round shape.

Thermal analysis of the UV-cured VSMP was carried out using a model DSC 4000 by PerkinElmer (MA, USA). A small piece of the specimen (7.26 mg) was placed in an aluminum pan and scanned between 0 and 200 °C with heating and cooling rates of 10 °C min⁻¹. The purging rate of the nitrogen gas is 30 mL min⁻¹.

Thermomechanical testing of the UV-cured VSMP specimen (6.16 × 18.63 × 1.11 mm) was conducted using a model Q800 DMA (TA Instruments, DE, USA) in the multi-frequency-strain mode with a 3 °C min⁻¹ temperature ramp rate, 0 to 180 °C temperature scan range, 15 μm amplitude, and 1 Hz frequency.

2.5 Recycling

The UV-cured VSMP (40 g) was first manually broken into small pieces and then added into the ceramic containers of the ball milling machine (Across International PQ-N2 Planetary, Livingston, New Jersey, USA). The broken pieces were then ground into particles through ball milling at room temperature for 20 h. The particles were added into a steel mold (Fig. S7(A)†), and the recycling process was carried out by applying a high pressure (6–14 MPa) on the steel mold at 130–175 °C for 2 h. By removing the bottom of the steel mold and compressing the pushing bar, a dark brown specimen (4.21 × 4.98 × 59.99 mm) was obtained. Three recycling cycles in total were carried out. The specimen recycled from the previous cycle was ground into powder again *via* ball milling and re-molded into a specimen for the new cycle. The recycling efficiency was assessed using eqn (2):

$$\text{Recycling efficiency} = \frac{\sigma_R}{\sigma_0} \times 100\% \quad (2)$$

where σ_R is the tensile strength of the recycled VSMP and σ_0 is the tensile strength of the initial VSMP before recycling.

2.6 SEM analysis

SEM microanalysis (Quanta 3D FEG, Hillsboro, OR, USA) was conducted to characterize the surface morphology of the

fracture surface of the VSMP specimen obtained from the ultimate tensile strength test and the morphology of the ground particles for recycling. The sample surfaces were coated with platinum approximately 6 nm thick. The accelerating voltage was 5 kV, and the working distance was 9–9.5 mm.

2.7 Shape memory effect and recovery stress

To test the shape memory effect, a cylindrical specimen made of BPAGMA (diameter = 12.27 mm, height = 19.20 mm). The cylindrical specimen underwent a hot programming process. It was placed into the MTS machine with the temperature increased to 150 °C, and the whole system stayed isothermal for 1 h to reach equilibrium. The compression programming started with compression at a rate of 0.25 mm min⁻¹ until 24% strain, followed by cooling down the whole MTS system to room temperature while holding the stress constant. After unloading at room temperature, the compression programming process was completed. Free shape recovery was conducted by heating the programmed VSMP to 150 °C without any load and staying isothermal for 15 min. The shape fixity ratio (F) and shape recovery ratio (R) were calculated using eqn (3) and (4), respectively:

$$F = \frac{\varepsilon_f}{\varepsilon_1} \times 100\%, \quad (3)$$

$$R = \frac{\varepsilon_f - \varepsilon_r}{\varepsilon_f} \times 100\% \quad (4)$$

where ε_1 is the measured strain before load removal, ε_f is the fixed strain after load removal, and ε_r is the residual strain after recovery.

To measure the recovery stress, the programmed cylinder was fully constrained by the fixtures of the MTS machine in a pre-heated oven (150 °C, 1 h) so that the thermal expansion of the metal fixtures can be avoided. Once the cylindrical specimen was confined, the data collection started to record the stress as a function of time. The relationship between the recovery stress and recovery strain was also investigated. When the recovery stress in the fully constrained recovery stress test was stabilized, we allowed 1.33% of recovery strain to occur by retreating the test fixture, and the recovery stress reduced until

stabilization. The next step repeated the same procedure of the previous step until the recovery stress became zero. The energy output was calculated based on the area under the curve of recovery stress and recovery strain.

3. Results and discussion

3.1 Study of curing kinetics

The kinetics of the polymerization conversion was first investigated. The kinetic profile shows similarity to the profile of a typical chain-growth radical polymerization. More than 60% crosslinking happens within only 10 s, and the polymerization conversion reaches 70% after 20 s with a decrease in the polymerization rate, due to the limited chain mobility within a bulk network compared to a solution. The conversion increases to nearly 100% after 80 s exposure to UV radiation, resulting in a highly constrained network (Scheme 1(a)). Because the crosslinking process propagates through UV-triggered radical polymerization, the crosslinking degree can be directly reflected by the polymerization conversion. The mechanical strength of the VSMP increases proportionally with the crosslinking degree from less than 20 MPa to 36 MPa when the crosslinking density increases from about 70% to about 80%, but it becomes almost independent of the crosslinking degree after 40 s exposure time. The specimen obtained at 80 s exposure has 36.7 MPa ultimate tensile strength (Fig. S1†). On the other hand, the ultimate strain of the VSMP exhibits a trend of slight decrease as a function of the crosslinking degree (Fig. 1(A)).

3.2 Compositional and thermomechanical analysis

The compositional analyses of the BPAGMA monomer and the UV-cured VSMP were conducted using FT-IR (Fig. 2). All the characteristic peaks are assigned to functional peaks (Table S1†). The UV-curing is suggested according to the decrease in the peak b at 1630 cm⁻¹, which corresponds to the -C=C- bond of the methacrylate functional group.

The thermal properties and thermomechanical properties of the UV-cured VSMP were analyzed by differential scanning calorimetry (DSC) and dynamic mechanical analysis (DMA), respectively. The DSC thermal analysis was conducted, but the

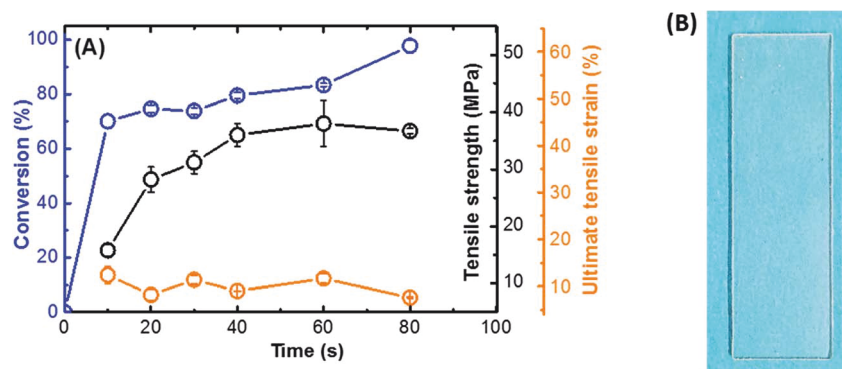


Fig. 1 (A) The plot of conversion, tensile strength, and ultimate tensile strain as a function of time. (B) The picture of the UV-cured VSMP.

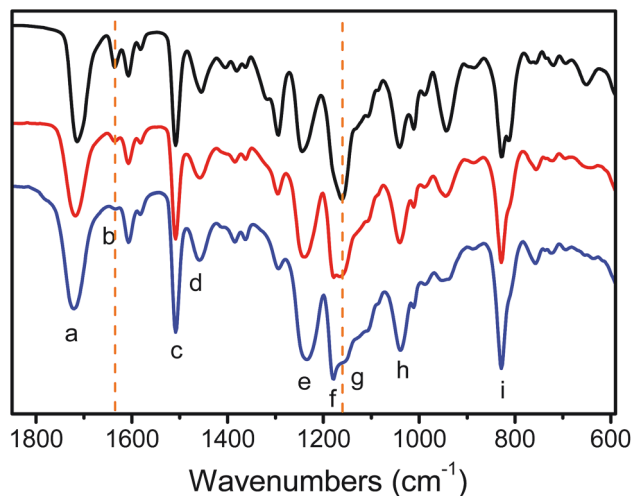


Fig. 2 Compositional analysis of the BPAGMA monomer (□), the UV-cured VSMP (□), and the recycled VSMP (□) by FT-IR.

thermal behaviors of the VSMP cannot be determined by DSC because only small bumps are seen in the thermograms. The peak of the first heating cycle with the onset point at 38 °C is probably due to the polymerization of a small amount of unreacted monomers, which disappeared in the second heating cycle (Fig. S2†). However, two T_g transition regions were revealed by the DMA analysis (Fig. 3): one peak of the tan delta curve is at 75 °C and the other one is at 158 °C, respectively. The cross-linking density throughout the VSMP specimen may be nonuniform due to the oxygen inhibition on the surface, resulting in the two T_g regions. The VSMP exhibits good thermal stability, evidenced by high stiffness in a wide temperature range. It has 3121 MPa storage modulus at room temperature and 1543 MPa storage modulus even at its first T_g temperature. Its storage modulus remains above 1000 MPa when the temperature is as high as 100 °C. It is noted that although the second DSC curve cannot clearly show the two T_g peaks due to the low resolution of the DSC device, the bumps still consist of some useful information. We calculated the first derivative of the DSC thermogram (2nd heating cycle) as a function of

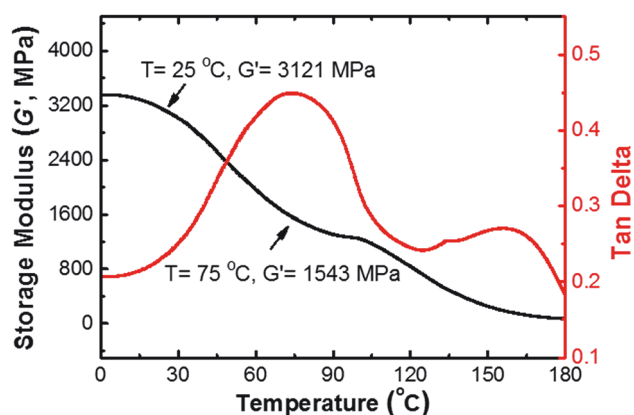


Fig. 3 Thermomechanical analysis of the UV-cured VSMP using DMA with 3 °C min⁻¹ temperature ramp rate.

temperature; see Fig. S3.† The first derivative curve has been employed to help determine the T_g when the resolution of the DSC thermogram is low.⁴⁵ The curve of the first derivative has three peaks, indicating that the T_g can be roughly 60 °C, 96 °C, and 158 °C. It should be noted that the scale of the DSC specimen is more than 10 times smaller than that of the DMA specimen (roughly 7 mg vs. 100 mg). Due to the nonuniform crosslinking, the result of DSC thermal analysis may vary a little as compared to that of the DMA analysis.

3.3 Mechanical tests and recyclability assessment

It has been shown before that a vitrimer-based epoxy thermoset may lose significant mechanical strength at elevated temperatures.²² Good thermal stability of the VSMP is always desired for high temperature engineering applications. The compressive behavior of the VSMP at elevated temperatures was investigated with cylindrical specimens fabricated through *in situ* UV-curing inside plastic syringes. The cylindrical VSMP exhibits good compressive strength (230 MPa) at room temperature (Fig. S4†). Interestingly, at 75 °C, the first T_g point measured by tan δ , the VSMP shows better compressive strength and strain (256 MPa, 43%) than at room temperature. The two T_g regions may be playing an important role in the increased compressive strength at 75 °C. At the first T_g point, some of the polymer segments are in the rubbery state, providing more flexibility to the VSMP. Meanwhile, a large amount of the VSMP segments are still in the glassy state, ensuring the high mechanical strength. Consequently, the VSMP at the first T_g point behaves like a composite with higher compressive strength than at room temperature. The good thermal compressive strength (187 MPa) is maintained until 120 °C, which is still higher than that of most plastics at room temperature (Fig. S4†).

The tensile strength of specimens with varying crosslinking degrees was investigated using a rectangular specimen (18.30 × 54.31 × 1.13 mm) (Fig. 1). The tensile strength reaches a plateau after the crosslinking degree comes to 80%. According to the representative stress vs. strain plot of the specimen cured at 80 s, there is no yielding of the material before it is broken due to the highly constrained network and high chain stiffness. The tensile strength at fracture is 36.7 MPa and the elongation is 8% (Fig. S1†). The SEM microanalysis of the fracture shows a smooth or a brittle fracture surface (Fig. S5†).

In order to investigate the recyclability of the UV-cured VSMP, the specimens cured at 80 s (40 g) were ground into white powders using a ball milling machine for 24 hours at room temperature (Fig. S6(A)†). The morphology and size distribution of the powder particles were analyzed using SEM (Fig. S6(B) and S6(C)†). It is shown that the powders are irregularly shaped particles with the size distribution ranging from around 0.5–3.8 μ m.

The ground powders were then recycled in a steel mold (Fig. S7(A)†) under a stress provided by the MTS machine at an elevated temperature (150 °C), which is around the second T_g . The elevated temperature enables the segment mobility of the CAN in the rubbery state, and the applied stress enhances the particle–particle contact and inter-diffusion of the polymer chains on the particle surface. IR analysis suggested that the

recycling process occurred *via* a transesterification reaction between the dangling hydroxyl groups and the ester bonds (Fig. 2). The decrease in the peak at 1158 cm^{-1} , which corresponds to the saturated C–O stretching of the VSMP, indicates the original ester bond breakage;⁴⁶ the formation of the new ester group is implied by the increase in the peak at 1183 cm^{-1} , which is related to a new C–O stretching (Scheme S1†).⁴⁷

A systematic study of the effect of recycling conditions on the recycling efficiency of an epoxy thermoset has been reported by our group, which indicates that all the three factors: applied stress, recycling temperature, and process time have effects on the recycling efficiency.⁴⁸ With respect to the recycling time, it only makes a big difference when it is increased from 2 h to 10 h. To pursue a more efficient recycling process, all the tests used the same 2 h recycling time. The effects of the applied stress and recycling temperature were investigated to find the optimal conditions. Once the recycling process was done, the re-molded specimen in dark orange color (Fig. S7(B)†) was removed from the mold and its tensile strength was tested (Fig. 4) and compared to the original tensile strength to obtain the recycling efficiency (RE).

It is shown that at a fixed temperature ($150\text{ }^{\circ}\text{C}$) the RE increases from 43.5% to 69.5% by increasing the applied stress from 6 MPa to 14 MPa, suggesting that the inter-diffusion process of the particle surface is a crucial factor. When the recycling temperature increases from $130\text{ }^{\circ}\text{C}$ to $150\text{ }^{\circ}\text{C}$, the RE increases due to a higher segment mobility and faster interfacial transesterification rate at $150\text{ }^{\circ}\text{C}$. By further increasing the recycling temperature to $175\text{ }^{\circ}\text{C}$, the RE does not increase but decreases by 14%. This may be due to a competing aging

process of the VSMP at an elevated temperature. Therefore, entry 3 (Table 1) shows the optimal recycling conditions for this VSMP.

Under the optimal recycling conditions, the recyclability was assessed by extending the number of recycling cycles. The mechanical strength of the recycled specimen was investigated by conducting the tensile strength test (Fig. 5), and the RE was calculated based on the same equation. For the first two recycling cycles, the RE remained above 60%, and the specimen obtained from the second recycling cycle has the same appearance as the specimen obtained from the first recycling cycle (Fig. S7(B)†). However, the specimen obtained from the third recycling cycle has a much darker color than the first two (Fig. S7(B)†), and its RE has a considerable decrease to only 25.3%, indicating that the VSMP can be effectively recycled and reused twice with more than 60% tensile strength of the original VSMP (Table 2). With 62% RE, the tensile strength is about 23 MPa, which is comparable to that of the commercial high impact polystyrene.

3.4 Shape memory effect

The shape recovery ratio and recovery stress of the UV-cured VSMP were tested by following two 5-step procedures, respectively. The first four steps for the two procedures are the same: (1) heating up the system, (2) loading at the rubbery temperature, (3) cooling to a glassy state while holding the stress constant, and (4) unloading (Fig. 6). To briefly introduce this process, a small cylinder (diameter 12.27 mm and height 19.20 mm) made of the UV-cured VSMP was compressed using

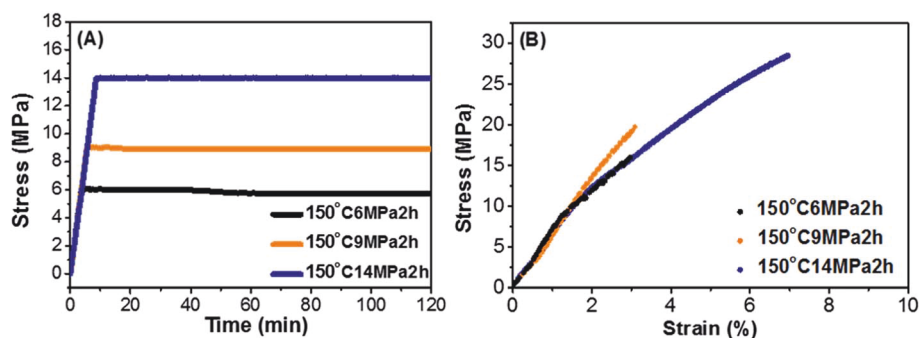


Fig. 4 (A) Representative plots of the externally applied stress on the steel mold containing the ground VSMP powders as a function of time during the recycling processes. (B) Representative plots of the stress vs. strain curve of the recycled VSMPs under varying conditions.

Table 1 Summary of recycling results under various conditions

Entry	Conditions ^a	Tensile strength [MPa]	Failure strain [%]	Recycling efficiency [%]
1	150°C/6MPa/2h	14.6 ± 1.3	3.8 ± 0.8	40.0
2	150°C/9MPa/2h	17.2 ± 2.6	4.4 ± 1.3	46.9
3	150°C/14MPa/2h	25.5 ± 4.0	9.7 ± 2.5	69.5
4	130°C/14MPa/2h	12.4 ± 0.1	1.7 ± 0.4	33.8
5	175°C/14MPa/2h	19.3 ± 1.0	3.6 ± 1.4	52.6

^a 150°C/6MPa/2h means recycling at $150\text{ }^{\circ}\text{C}$ and under 6 MPa pressure for 2 hours.

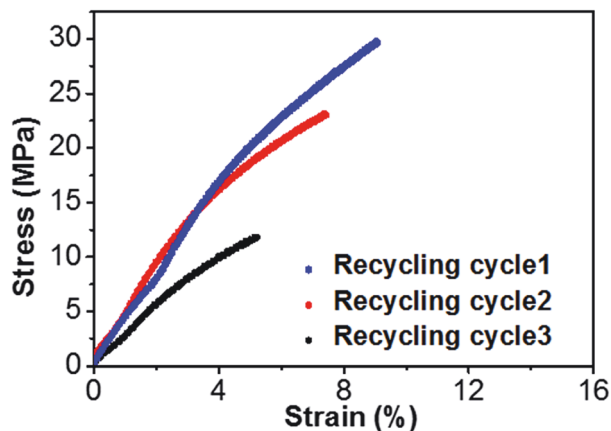


Fig. 5 Representative plots of stress vs. strain of the specimens obtained from three recycling cycles, respectively.

Table 2 Summary of mechanical properties and recycling efficiency after each recycling cycle

Cycle	Tensile strength [MPa]	Failure strain [%]	Recycling efficiency [%]
1	25.5 ± 4.0	9.7 ± 2.5	69.5
2	22.8 ± 0.5	5.9 ± 1.0	62.1
3	9.3 ± 3.8	6.9 ± 4.3	25.3

the MTS machine at 150 °C in an oven which was pre-heated for 1 h. The cooling step started right after the loading step to freeze the mobility of the chain segments of the VSMP so that the temporary deformation can be fixed. It is shown that about 27 MPa was needed to compress the cylinder at 150 °C for 24% strain. The stress was maintained the same at 0 N min⁻¹ loading rate during the cooling process, and it became zero after removing the external load at room temperature, which is

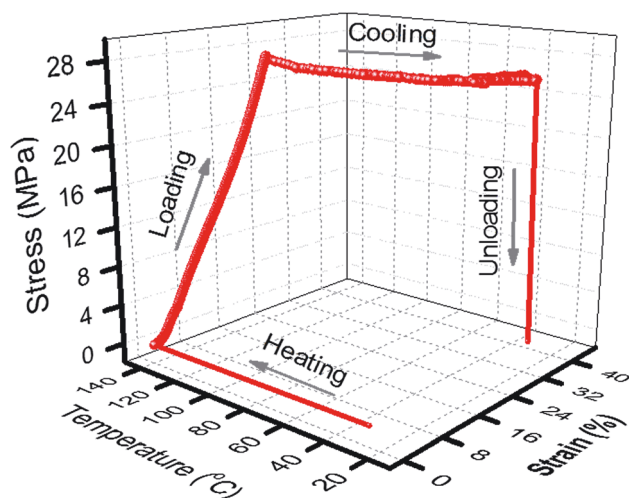


Fig. 6 A representative 4-step programming profile of the UV-cured VSMP at 150 °C with 0.25 mm min⁻¹ compression rate.

the 4th step – unloading (Fig. 6). The shape fixity ratio (F) is obtained by comparing the height of the specimen after unloading to the height of the cooled specimen under load (eqn (3)). Free shape recovery was achieved by placing a programmed specimen in the MTS oven and then increasing the temperature from room temperature to 150 °C. The shape recovery ratio (R) was obtained using eqn (4). Table 3 gives the F and R obtained for at least four shape recovery cycles.

To avoid the effect of thermal expansion of the MTS fixtures on the shape recovery stress, the MTS system was pre-heated at 150 °C for 1 h. The recovery stress was measured by confining a programmed cylinder (diameter 13.87 mm and height 15.39 mm) using the MTS fixtures. The maximum recovery stress was first recorded with zero recovery strain (Fig. S8†). The programmed cylinder exhibits a rapid stress recovery which takes only 4 min to reach 9.4 MPa recovery stress and 9 min to reach a large recovery stress of 13 MPa. The recovery stress eventually stabilizes at 13.4 MPa after about 16 min and remains constant for more than 1 h. Some of the reported maximum recovery stress values of various SMPs have been summarized (Fig. S9†). Many other SMPs also show less than 2 MPa of recovery stress, which can be found in ref. 25. It can be seen that the recovery stress of the VSMP is even higher than some of the carbon nanotube (CNT) reinforced SMPs. To the best of our knowledge, the epoxy VSMP is so far the only known vitrimer with stabilized recovery stress higher than 10 MPa.

The relationship between recovery stress and recovery strain was then investigated. It is shown that the recovery stress decreases as the recovery strain increases (Fig. 7). The programmed cylinder is able to produce a large and stabilized recovery stress (more than 6 MPa) with 8% recovery strain. Moderate recovery stress (3 to 5 MPa) can be produced and maintained with 8% to 12% recovery strain. The study of recovery stress as a function of recovery strain shows that the VSMP can yield a large and stable stress in the real world working conditions. The energy output of the UV-cured VSMP was calculated based on the area under the curve of recovery stress vs. recovery strain, showing that 1.05 MJ m³ energy output can be produced throughout the whole stress recovery process.

Normally, epoxy-based SMPs which usually produce low to moderate recovery stress (less than 5 MPa) require a curing agent to connect the hard epoxy segments. In contrast, the UV-cured VSMP is fabricated through a complete radical polymerization without any curing agent, and the BPAGMA hard segments can be directly connected to each other and produce a highly constrained network, leading to the large recovery stress and energy output.

Table 3 Summary of the shape fixity ratio and the shape recovery ratio after multiple shape recovery cycles

Recovery cycle	1	2	3	4
Shape fixity ratio (F) [%]	100	94.3	98.1	93.2
Shape recovery ratio (R) [%]	99.0	100	100	96.9

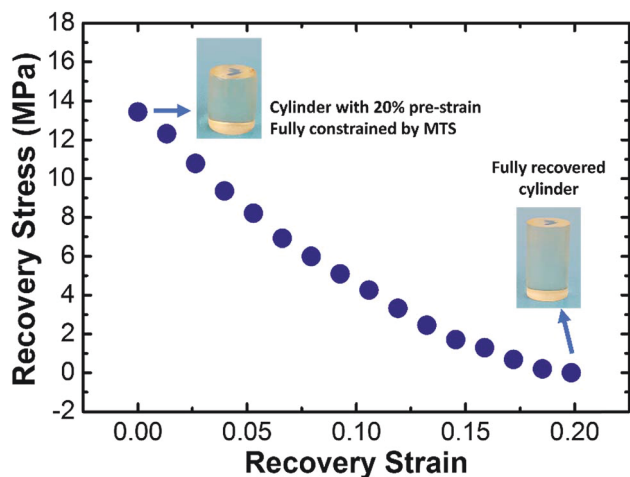


Fig. 7 Profile of the recovery stress vs. recovery strain which is measured using the MTS machine at 150 °C using the programmed VSMP cylinder (diameter 13.87 mm and height 15.39 mm).

4. Conclusions

Three main issues that restrict the engineering applications of current HPSMPs are their complex fabrication processes, lack of recyclability, and low recovery stress and energy output. To address all the critical issues simultaneously, a UV-curable and recyclable thermoset VSMP with high stress and energy output was synthesized, which can be prepared under UV irradiation in just 80 s at room temperature. The VSMP exhibits high mechanical properties (tensile strength = 36.7 MPa, ultimate tensile strain = 8%, compressive strength = 230 MPa, and storage shear modulus is about 3000 MPa) at room temperature. Good thermal stability of the VSMP has been demonstrated by its compressive behavior at elevated temperature (compressive strength = 187 MPa at 120 °C). The recyclability of the SMP was investigated by grinding the thermoset into small particles *via* ball milling. Optimal recycling conditions were found (at 150 °C and under 14 MPa pressure for 2 hours), which led to more than 60% recycling efficiency for two recycling cycles. The future work will further focus on improving the recycling efficiency and recycling cycles. In addition, the SMP possesses good shape memory effect for multiple shape recovery cycles. Due to its highly constrained network, comparatively large shape recovery stress up to 13.4 MPa can be obtained with 1.05 MJ m⁻³ energy output in the rubbery state. The new multifunctional VSMP may be used as adhesives, coatings, 3D printing inks, and actuators to broaden the applications of the HPSMP in engineering.

Conflicts of interest

There are no conflicts to declare.

Acknowledgements

The authors gratefully acknowledge the financial support by National Science Foundation under grant number 1333997 and

1736136, and NASA cooperative agreement NNX16AQ93A under contract number NASA/LEQSF(2016–19)-Phase3-10.

References

- P. T. Mather, X. Luo and I. A. Rousseau, *Annu. Rev. Mater. Res.*, 2009, **39**, 445–471.
- G. Li and A. Wang, *J. Polym. Sci., Part B: Polym. Phys.*, 2016, **54**, 1319–1339.
- A. Lendlein, H. Jiang, O. Jünger and R. Langer, *Nature*, 2005, **434**, 879–882.
- J. W. Cho, J. W. Kim, Y. C. Jung and N. S. Goo, *Macromol. Rapid Commun.*, 2005, **26**, 412–416.
- R. Mohr, K. Kratz, T. Weigel, M. Lucka-Gabor, M. Moneke and A. Lendlein, *Proc. Natl. Acad. Sci. U. S. A.*, 2006, **103**, 3540–3545.
- Z. Yu, Q. Zhang, L. Li, Q. Chen, X. Niu, J. Liu and Q. Pei, *Adv. Mater.*, 2011, **23**, 664–668.
- T. Ware, D. Simon, K. Hearon, C. Liu, S. Shah, J. Reeder, N. Khodaparast, M. P. Kilgard, D. J. Maitland and R. L. Rennaker, *Macromol. Mater. Eng.*, 2012, **297**, 1193–1202.
- H. Lu, K. Yu, Y. Liu and J. Leng, *Smart Mater. Struct.*, 2010, **19**, 065014.
- R. Akashi, H. Tsutsui and A. Komura, *Adv. Mater.*, 2002, **14**, 1808–1811.
- Y. Y. Chan Vili, *Text. Res. J.*, 2007, **77**, 290–300.
- A. Lendlein and R. Langer, *Science*, 2002, **296**, 1673–1676.
- G. Li, *Self-healing Composites: Shape Memory Polymer Based Structures*, John Wiley & Sons, 2014.
- A. D. Taleghani, G. Li and M. Moayeri, *J. Energy Resour. Technol.*, 2017, **139**, 062903.
- W. M. Sokolowski and S. C. Tan, *J. Spacecr. Rockets*, 2007, **44**, 750.
- X. Qi, G. Yang, M. Jing, Q. Fu and F.-C. Chiu, *J. Mater. Chem. A*, 2014, **2**, 20393–20401.
- Y. Liu, J. Zhao, L. Zhao, W. Li, H. Zhang, X. Yu and Z. Zhang, *ACS Appl. Mater. Interfaces*, 2015, **8**, 311–320.
- T. Zhang, Z. Wen, Y. Hui, M. Yang, K. Yang, Q. Zhou and Y. Wang, *Polym. Chem.*, 2015, **6**, 4177–4184.
- Q. Wang, Y. Bai, Y. Chen, J. Ju, F. Zheng and T. Wang, *J. Mater. Chem. A*, 2015, **3**, 352–359.
- Y. Bai, Y. Chen, Q. Wang and T. Wang, *J. Mater. Chem. A*, 2014, **2**, 9169–9177.
- C. Likitaporn, P. Mora, S. Tiptipakorn and S. Rimdusit, *J. Intell. Mater. Syst. Struct.*, 2017, **29**, 388–396.
- C. Véchambre, A. Buléon, L. Chaunier, C. Gauthier and D. Lourdin, *Macromolecules*, 2011, **44**, 9384–9389.
- L. Lu, J. Fan and G. Li, *Polymer*, 2016, **105**, 10–18.
- D. Santiago, A. Fabregat-Sanjuan, F. Ferrando and S. De la Flor, *J. Polym. Sci., Part B: Polym. Phys.*, 2016, **54**, 1002–1013.
- S. Hashmi, H. C. Prasad, R. Abishera, H. N. Bhargaw and A. Naik, *Mater. Des.*, 2015, **67**, 492–500.
- M. Anthamatten, S. Roddecha and J. Li, *Macromolecules*, 2013, **46**, 4230–4234.
- J. Fan and G. Li, *Nat. Commun.*, 2018, **9**, 642.
- K. Studer, C. Decker, E. Beck and R. Schwalm, *Prog. Org. Coat.*, 2003, **48**, 92–100.

- 28 J. Fouassier, *Radiat. Curing Polym. Sci. Technol.*, 1993, **1**, P49.
- 29 X. Luo and P. T. Mather, *ACS Macro Lett.*, 2013, **2**, 152–156.
- 30 R. Wang and T. Xie, *Langmuir*, 2010, **26**, 2999–3002.
- 31 L. Huang, R. Jiang, J. Wu, J. Song, H. Bai, B. Li, Q. Zhao and T. Xie, *Adv. Mater.*, 2017, **29**, 1605390.
- 32 M. Zarek, M. Layani, I. Cooperstein, E. Sachyani, D. Cohn and S. Magdassi, *Adv. Mater.*, 2016, **28**, 4449–4454.
- 33 X. Mu, T. Bertron, C. Dunn, H. Qiao, J. Wu, Z. Zhao, C. Saldana and H. Qi, *Mater. Horiz.*, 2017, **4**, 442–449.
- 34 C. J. Kloxin, T. F. Scott, B. J. Adzima and C. N. Bowman, *Macromolecules*, 2010, **43**, 2643–2653.
- 35 P. Zhang and G. Li, *Prog. Polym. Sci.*, 2016, **57**, 32–63.
- 36 A. B. Ihsan, T. L. Sun, T. Kurokawa, S. N. Karobi, T. Nakajima, T. Nonoyama, C. K. Roy, F. Luo and J. P. Gong, *Macromolecules*, 2016, **49**, 4245–4252.
- 37 B. Jin, H. Song, R. Jiang, J. Song, Q. Zhao and T. Xie, *Sci. Adv.*, 2018, **4**, eaao3865.
- 38 A. Li and D. Zhang, *Biomacromolecules*, 2016, **17**, 852–861.
- 39 Z. Fang, N. Zheng, Q. Zhao and T. Xie, *ACS Appl. Mater. Interfaces*, 2017, **9**, 22077–22082.
- 40 T. Defize, R. Riva, J. M. Thomassin, M. Alexandre, N. V. Herck, F. D. Prez and C. Jérôme, *Macromol. Rapid Commun.*, 2017, **38**, 1600517.
- 41 J. Bai and Z. Shi, *ACS Appl. Mater. Interfaces*, 2017, **9**, 27213–27222.
- 42 D. Wang, J. Guo, H. Zhang, B. Cheng, H. Shen, N. Zhao and J. Xu, *J. Mater. Chem. A*, 2015, **3**, 12864–12872.
- 43 E. D. Rodriguez, X. Luo and P. T. Mather, *ACS Appl. Mater. Interfaces*, 2011, **3**, 152–161.
- 44 J. Chauvet et, J. M. Asua and J. R. Leizaet, *Polymer*, 2005, **46**, 9555–9561.
- 45 M. M. Mok, J. Kim, C. Wong, S. R. Marrou, D. J. Woo, C. M. Dettmer, S. T. Nguyen, C. J. Ellison, K. R. Shull and J. M. Torkelson, *Macromolecules*, 2009, **42**, 7863–7876.
- 46 E. G. Chatzi, O. Kammona, A. Kentepozidou and C. Kiparissides, *Macromol. Chem. Phys.*, 1997, **198**, 2409–2420.
- 47 E. Sharmin, L. Imo, S. Ashraf and S. Ahmad, *Prog. Org. Coat.*, 2004, **50**, 47–54.
- 48 L. Lu, J. Pan and G. Li, *J. Mater. Chem. A*, 2017, **5**, 21505–21513.

Recyclable Epoxy Thermoset Shape Memory Polymer with High Stress and Energy Output via Facile UV-Curing

Ang Li, Jizhou Fan, and Guoqiang Li*

Department of Mechanical and Industrial Engineering, Louisiana State University, Baton Rouge,
Louisiana USA 70803

*Corresponding author: lguoqi1@lsu.edu (Dr. G. Li)

SUPPORTING INFORMATION

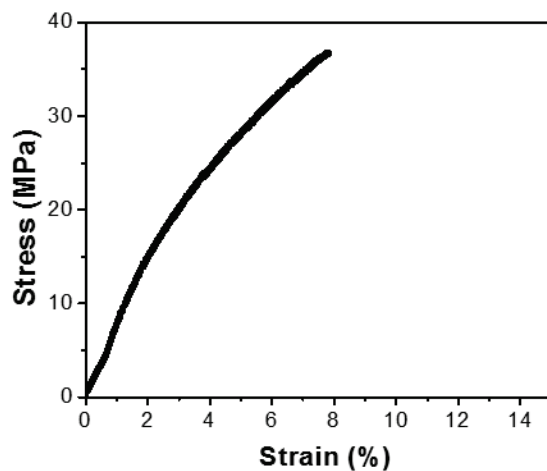


Figure S1. Typical plot of tensile stress vs. strain of the UV-cured thermoset VSMP specimen after 80 s curing time.

Table S1. Assignment of the characteristic peaks of the FT-IR spectrum in Figure 2.

Peak	Frequency	Attribution
a	1720	Ester carbonyl C=O stretch
b	1630	Double bond C=C
c	1506	Aromatic C=C stretch ¹
d	1452	Aromatic C=C stretch ¹
e	1243	Asymmetric C-O stretch ¹
f	1183	-O-CH ₂ -CH-O- stretch ²
g	1158	Saturated -CH ₂ -O- Stretch ³
h	1036	Symmetric C-O stretch ¹
i	829	Aliphatic C-O stretch

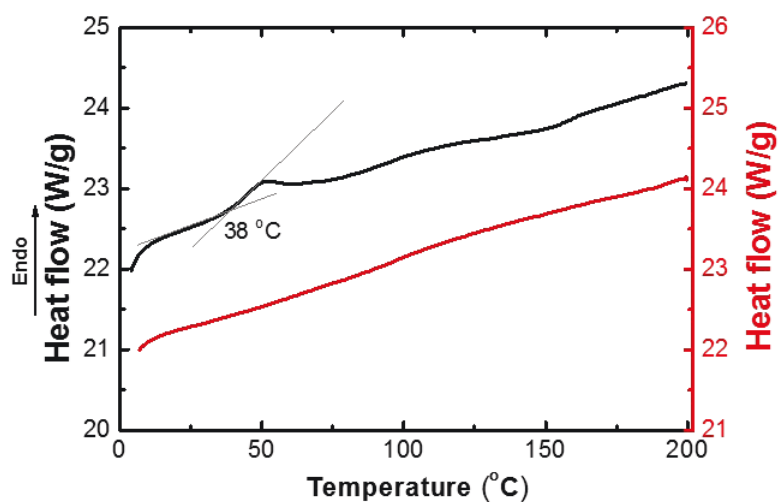


Figure S2. Thermograms of UV-cured thermoset VSMP. Black color represents the thermogram of the first heating cycle; Red color represents the thermogram of the second heating cycle.

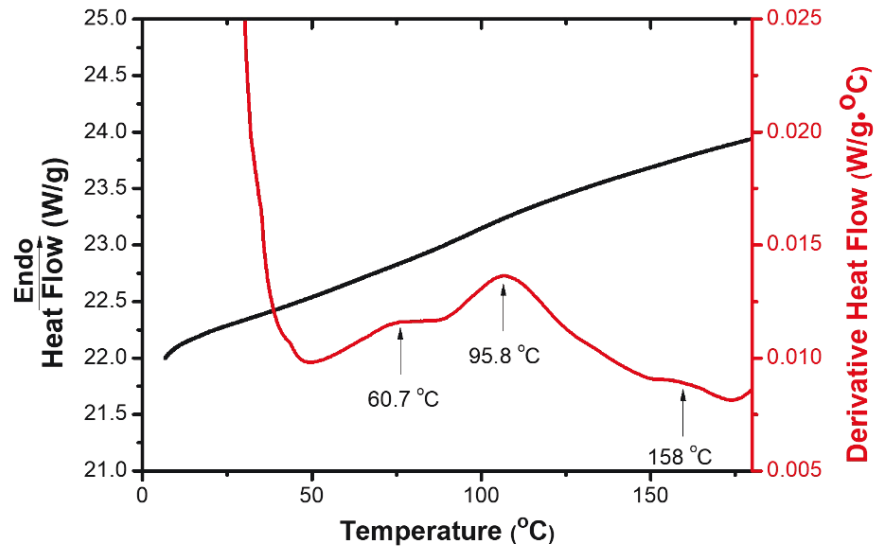


Figure S3. The first derivative of the heat flow with respect to temperature based on the second heating branch of the DSC test results

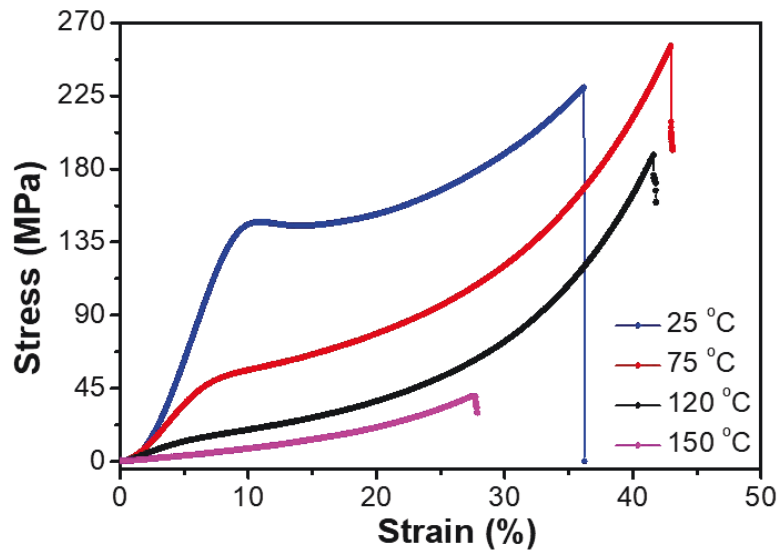


Figure S4. Representative compression behavior of the cylindrical VSMP specimens at room temperature and elevated temperatures.

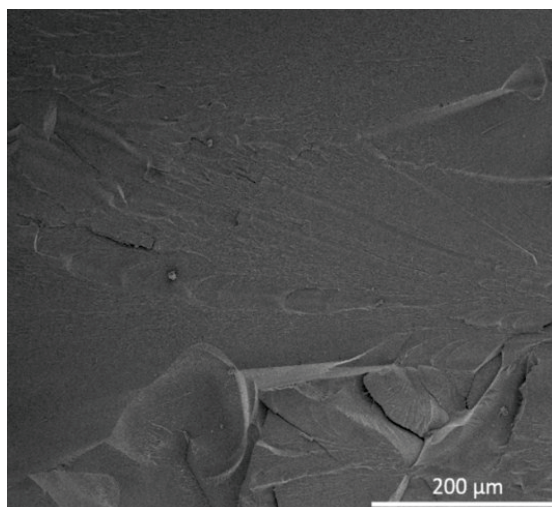


Figure S5. SEM image of the fracture surface of the UV-cured thermosets.

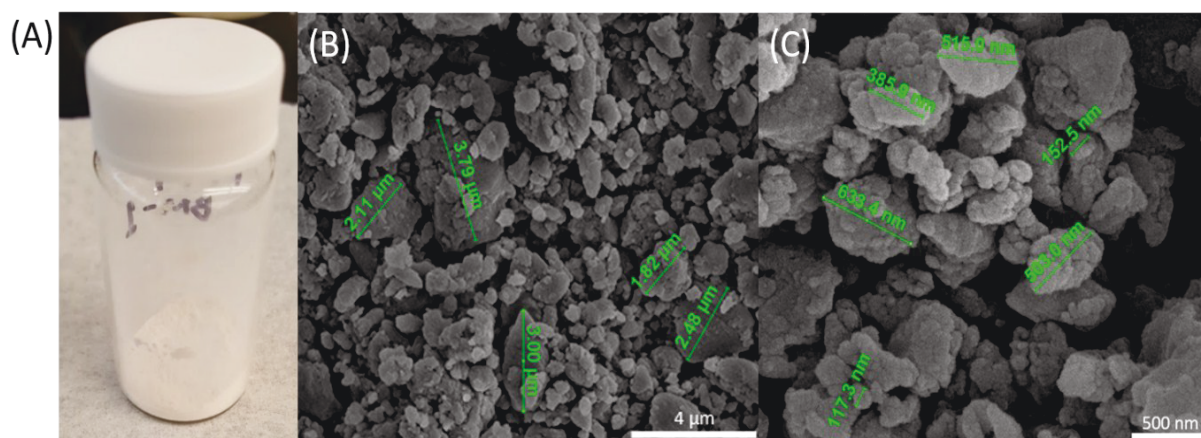


Figure S6. (A) Picture of the powder of the UV-cured thermoset ground by a ball milling machine. (B) SEM micrograph of the ground powder with powder size measured. (C) Zoom-in of the SEM micrograph of the ground powder.

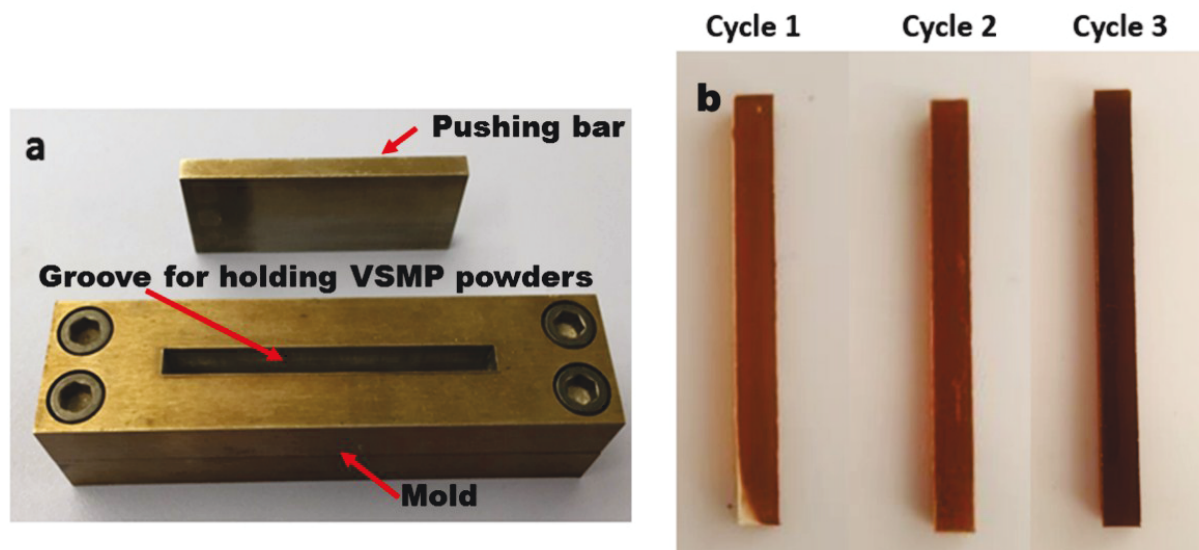
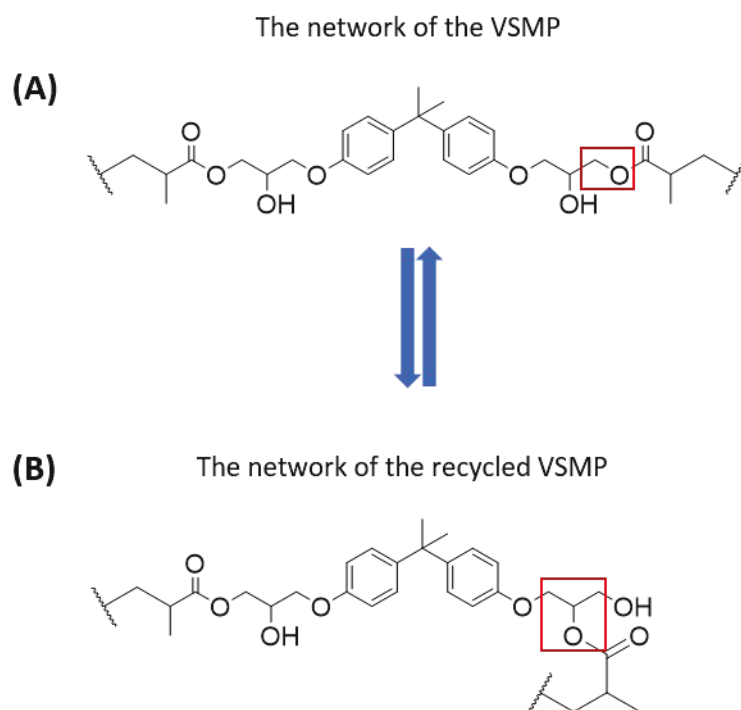


Figure S7. (A) The steel mold (bottom) and pushing bar (top) for preparing recycling VSMP specimens and (B) Representative pictures of the recycled thermoset specimen after the solid form recycling of the ground particles.



Scheme S1. (A) The transesterification reaction of the VSMP powders during the recycling process (150°C/14MPa/2h), (B) a possible network of the recycled VSMP.

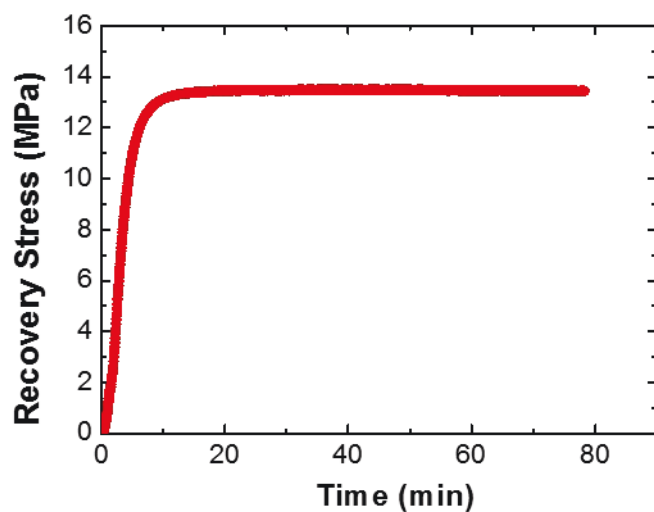


Figure S8. Representative profile of recovery stress vs. times measured by fully confining a cylindrical specimen (diameter = 12.28 mm, height = 19.20 mm) at 150 °C.

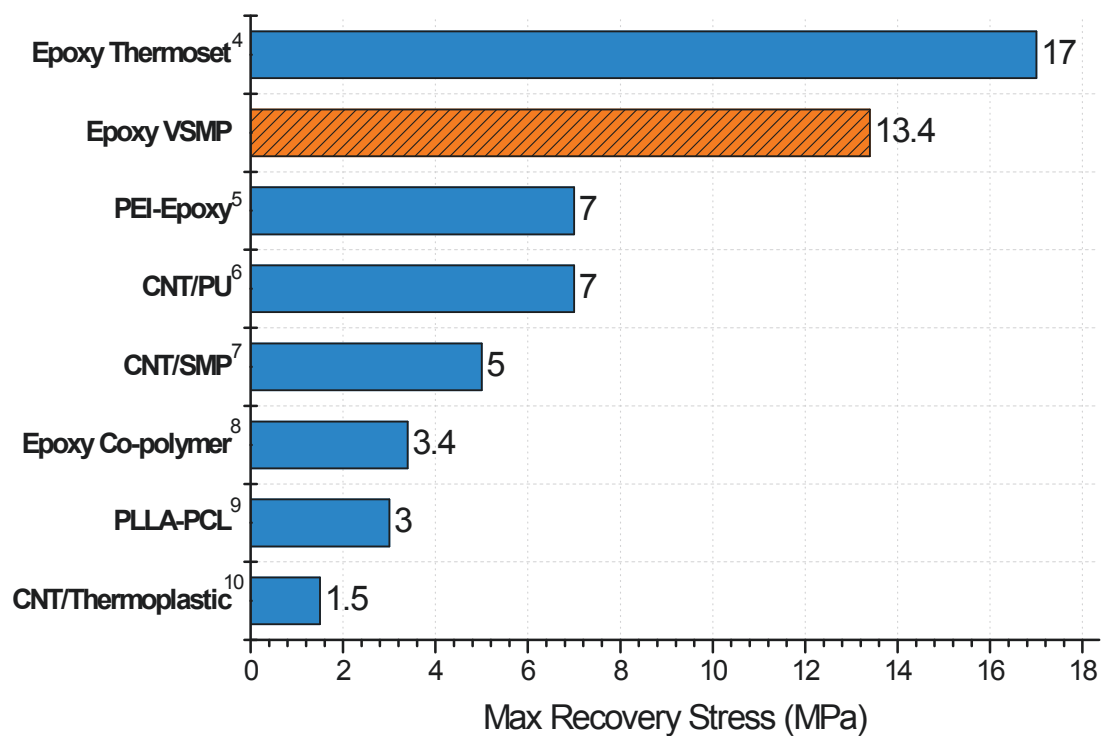


Figure S9. Reported maximum recovery stress of various shape memory polymers.

References:

1. Cherdoud-Chihani, A.; Mouzali, M.; Abadie, M. *J. Appl. Polym. Sci.* 2003, **87**, 2033-2051.
2. Sharmin, E.; Imo, L.; Ashraf, S.; Ahmad, S. *Prog. Org. Coat.* 2004, **50**, 47-54.
3. Chatzi, E. G.; Kammona, O.; Kentepozidou, A.; Kiparissides, C. *Macromol. Chem. Phys.* 1997, **198**, 2409-2420.
4. Fan, J.; Li, G. *Nat. Commun.* 2018, **9**, 642.
5. Santiago, D.; Fabregat-Sanjuan, A.; Ferrando, F.; De la Flor, S. *J. Polym. Sci., Part B: Polym. Phys.* 2016, **54**, 1002-1013.
6. Hashmi, S. A. R.; Prasad, H. C.; Abishera, R.; Bhargaw, H. N.; Naik, A. *Mater. Des.* 2015, **67**, 492-500.
7. Ni, Q. Q.; Zhang, C. S.; Fu, Y.; Dai, G.; Kimura, T. *Compos. Struct.* 2007, **81**, 176-184.
8. Likitaporn, C.; Mora, P.; Tiptipakorn, S.; Rimdusit, S. *J. Intell. Material Syst. Struct.*, 2017, 1045389X17708041.
9. Lu, X. L.; Sun, Z. J.; Cai, W.; Gao, Z. Y. *J. Mater. Sci. Mater. Med.* 2008, **19**, 395-399.
10. Koerner, H.; Price, G.; Pearce, N. A.; Alexander, M.; Vaia, R. A. *Nat. Mater.* 2004, **3**, 115.